Developmental Origin and Identity of Song System Neurons Born during Vocal Learning in Songbirds

BENJAMIN B. SCOTT AND CARLOS LOIS*

Department of Brain and Cognitive Sciences, Picower Institute for Learning and Memory, MIT, Cambridge, Massachusetts 02139

ABSTRACT

New neurons are added to the forebrain song control regions high vocal center (HVC) and Area X of juvenile songbirds but the identity and site of origin of these cells have not been fully characterized. We used oncoretroviral vectors to genetically label neuronal progenitors in different regions of the zebra finch lateral ventricle. A region corresponding to the mammalian medial and lateral ganglionic eminences generated medium spiny neurons found in Area X and in the striatum surrounding Area X, and at least two classes of interneurons found in HVC. In addition, our experiments indicate that the HVC projection neurons that project into nucleus robust nucleus of the arcopallium (RA) are born locally from the ventricular region immediately dorsal to HVC. The ability to genetically target neuron subpopulations that give rise to different song system cell types provides a tool for specific genetic manipulations of these cell types. In addition, our results suggest striking similarities between neurogenesis in the embryonic mammalian brain and in the brain of the juvenile songbird and provide further evidence for the existence of conserved cell types in the forebrain for birds and mammals. J. Comp. Neurol. 502:202–214, 2007. © 2007 Wiley-Liss, Inc.

Indexing terms: neurogenesis; basal ganglia; medium spiny neuron; interneuron; critical period; zebra finch

The songbird brain contains a neural pathway specialized for the production of learned vocalizations (Nottebohm, 1999). This pathway, termed the song system, consists of interconnected song nuclei located in the forebrain, midbrain, and hindbrain dedicated to processing auditory and motor signals related to song. The song system is not fully formed during the embryonic stage. Instead, it undergoes dramatic anatomical development while juvenile songbirds learn their song. During the song learning period, two song nuclei of the juvenile male songbird forebrain, the high vocal center of the nidopallium (HVC) and Area X of the striatum, greatly increase in neuron number (Nordeen and Nordeen, 1988, 1990; Alvarez-Buylla et al., 1988a). New neurons are also added to these two nuclei in adulthood, particularly at the time when the song is modified. The temporal relationship between new neuron addition and song learning has lead to the hypothesis that postnatal neurogenesis plays an important role in song learning (Alvarez-Buylla et al., 1990a; Nottebohm, 2002; Wilbrecht et al., 2006). However, the identity of the neurons added to the song system after hatching has been only partially characterized (Alvarez-Buylla et al., 1990a;

Kirn et al., 1991; Sohrabji et al., 1993; Nordeen and Nordeen, 1988; Nottebohm, 2004) and detailed knowledge about their morphology, electrophysiology, and connectivity is needed to formulate realistic hypotheses about the function of postnatal neurogenesis in the songbird brain.

Telencephalic neural progenitors are known to reside in the ventricular zone (VZ) in the walls of the lateral ventricles during vertebrate embryonic development. Different subregions of the VZ are specialized for the production of different classes of neurons. The VZ of the lateral ventricle can be divided during the embryonic stage into two

The Journal of Comparative Neurology. DOI 10.1002/cne

NEUROGENESIS IN SONGBIRDS 203

regions, the pallial VZ and subpallial VZ, each specialized for the production of different classes of neurons. The pallial VZ, which lies adjacent to the pallial anlage, expresses the T-box transcription factor TBR1 and, in mice, generates excitatory neurons of the cortex (Hevner et al., 2006). The subpallial VZ, which is adjacent to the striatal anlage, expresses the homeobox gene DLX2, and in mice gives rise to inhibitory interneurons in the striatum and cortex as well as the medium spiny neurons (MSNs) of the striatum (Marin and Rubenstein, 2003). In mammals the VZ is a transient structure that exists during a brief period during embryogenesis. In birds the VZ persists after birth (Alvarez-Buylla et al., 1998) and is thought to continue to produce new neurons into adulthood (Goldman and Nottebohm, 1983; Alvarez-Buylla and Nottebohm, 1988; Alvarez-Buylla et al., 1990a; Dewulf and Bottjer, 2005); however, the different cell types produced by the VZ after hatching remain unknown.

We sought to characterize the postnatal VZ of juvenile zebra finches and to determine the developmental origin and identity of the new neurons added to the song system. We performed immunohistochemical analysis of TBR1 and DLX expression to identify the pallial and subpallial VZ. We then used local injections of an oncoretroviral vector carrying the gene for the green fluorescent protein (GFP) to label neuronal progenitors in subregions of the VZ expressing either TBR1 or DLX genes. Thirty-five days after infection of the lateral ventricle we observed mature, GFP-positive (GFP+) neurons in HVC and Area X. Neurons in HVC that extended axons into the robust nucleus of the arcopallium (RA) appeared following the infection of the TBR1-positive (TBR1+) VZ overlying HVC. After infection of the DLX-positive (DLX+) VZ adjacent to the striatum, a region homologous to the mammalian medial ganglionic eminence (MGE) and lateral ganglionic eminence (LGE) (Puelles et al., 2000), medium spiny neurons were detected in Area X and two types of GABAergic neurons were detected in HVC.

These observations have allowed us to characterize the phenotype of the new neurons that are added into juvenile brain nuclei of the song system during the period of song learning. In addition, the identification of the site of origin of these different neuron types provides us with a convenient method to genetically manipulate the activity of song system cells. Finally, our observations reveal striking homologies between brain development in embryonic mammals and juvenile songbirds, and suggests that the array of cell types in the avian and mammalian forebrain is more similar than previously thought.

MATERIALS AND METHODS
Viral vectors

Oncoretroviral vectors based on the Moloney Murine Leukemia Virus were engineered to carry GFP under control of the internal promoter of the Rous Sarcoma Virus (Yamamoto et al., 1980), which we determined to be a strong ubiquitous promoter in zebra finch cells. Viral vectors were pseudotyped with the VSVg envelope, produced as described for lentiviruses (Lois et al., 2002) and concentrated to 10^6 infectious units (I.U.)/μL. Following concentration, vector solutions were aliquoted and stored at $-80°$C.

Surgery

Zebra finches were obtained from our breeding colony at MIT. Twelve males were injected bilaterally into either the subpallial or pallial VZs 28–48 days after hatching. Bilateral injections were also made into the pallial VZs of four adult females. Stereotaxic coordinates used were based on the expression of marker proteins TBR1 and the DLX family and initially determined using stereotaxic coordinates derived from the canary atlas of Stokes et al. (1974) and subsequently confirmed empirically. The head of the bird was placed in a stereotaxic head holder at an angle of 45° and we defined the branch point of the sagittal sinus that lies just anterior to the rostral tip of the cerebellum as stereotaxic point 0.0 both for the anteroposterior and the mediolateral axes. To target the subpallial VZ we used the following coordinates: 1.6 mm anterior, 4.4–4.8 mm lateral, 3.75–3.85 mm bellow the dura and an injection angle tilted 45° relative to the horizontal plane. To target the VZ just dorsal to HVC we penetrated the brain perpendicular to the surface of the brain (90° vertical injection angle relative to the horizontal plane) and used the following coordinates: 0.3 mm anterior, 2.2 mm lateral, 0.17–0.3 mm deep.

Injection needles were constructed from pulled borosilicate capillary tubes (Sutter Instrument, Novato, CA) with a fine taper, whose tip had been cut to 20–50 μm inner diameter using a ceramic cutting tile (Sutter Instrument). Then 100–1,000 nL of vector solution was delivered by slow (0.5 nL per second) injection using a micropump (WPI, Sarasota, FL). Following surgery, animals were returned to our colony where they were housed with their family (if younger than 40 days posthatch) or other juvenile males (if older than 40 days posthatch).

For retrograde tracing of HVC$_{RA}$ projection cells, we injected 30 nL of FluoroGold (Fluorochrome, Englewood, CO) in the right RA and 30 nL of cholera toxin subunit B conjugated to Alexa Fluor 555 (Molecular Probes, Eugene, OR) in the left RA. FluoroGold was used as a tracer to allow comparison with previous studies that used this tracer. Cholera toxin subunit B conjugated to Alexa Fluor 555 was used to allow visualization of these cells by confocal microscopy. These injections were performed 7 days prior to perfusion. One juvenile zebra finch became ill 4 days after the RA injections and was perfused immediately. Previous studies have shown that 4 days are sufficient for retrograde tracing and we noticed no difference in the percentage of GFP+ cells retrogradely labeled in this animal or in the morphology of GFP+ cells.

Histology and immunohistochemistry

Juvenile zebra finch males were deeply anesthetized with ketamine and xylazine and perfused intracardially with 20 mL of phosphate-buffered saline (PBS), pH 7.4, followed by 3% paraformaldehyde in PBS (50 mL). Brains were removed from the skull and soaked in 3% paraformaldehyde for 12–24 hours at 4°C. After fixation, brains were washed with PBS and cut to 30, 50, or 100 μm sections with a vibrating microtome (Leica, Deerfield, IL).

Immunohistochemistry was performed with the following antibodies: NeuN was detected using a mouse monoclonal antibody (diluted in blocking solution 1:500) (Chemicon, Temecula, CA; MAB377, lot 19060600) raised against purified cell nuclei from the mouse brain. According to the manufacturer this antibody stains 2–3 bands in

the 46–48 kD range and 0–1 bands of molecular weight 66 kD on Western blot. Immunohistochemistry against NeuN is widely used to stain neurons; however, the identity of the antigen is not known. We used anti-NeuN to identify the borders of the song nuclei HVC and Area X. GABA was detected using a rabbit polyclonal antibody (diluted 1:2,000) (Sigma, St. Louis, MO; A2052, lot 095K4830) raised against GABA-BSA. According to the manufacturer this antibody shows positive binding to GABA and negative binding to BSA in a dot blot assay. Parvalbumin was detected using a mouse monoclonal antibody (diluted 1:1,000) (Sigma, P3088, lot 075K4794) raised against purified frog muscle parvalbumin. According to the manufacturer this antibody stains a 12-kD band on Western blot. DARPP-32 was detected using a mouse monoclonal antibody (diluted 1:10,000; clone C24-5a), a gift of H.C. Hemmings (Cornell University), raised against purified bovine DARPP-32. This antibody stains a single band of molecular weight 32 kD on Western blot (Hemmings and Greengard, 1986). A rabbit polyclonal antibody (diluted 1:1,000) against DLX family members was used to identify the subpallial portion of the juvenile zebra finch VZ. The antibody, a gift of S.B. Carroll (University of Wisconsin), was raised against a synthetic peptide corresponding to the following 61-amino acid homeodomain of butterfly DLL: MRKPRTIYSSLQLQQLNRRFQRTQYLALPERAE-LAASLGLTQTQVKIWFQNRRSKYKKMMK. This antibody recognizes a conserved homeodomain found in DLL and DLX proteins in arthropods (Panganiban et al., 1995) and vertebrates (Brown et al., 2005). TBR1 was detected using a rabbit polyclonal antibody (diluted 1:100), a gift of M. Sheng (MIT), raised against a synthetic peptide corresponding to residues 614–624 of mouse TBR-1 (Hsueh et al., 2000). This antibody has been shown to stain a band of molecular weight 85 kD in Western blots from mice and rat brains (Wang et al., 2004). The monoclonal antibody 39.4D5 (diluted 1:500), obtained from the Developmental Studies Hybridoma Bank (Iowa City, Iowa), was used to detect the region of the VZ putatively homologous to the mammalian lateral ganglionic eminence. This antibody was raised against a synthetic peptide corresponding to amino acid residues 178–349 of rat ISL-1 and has been shown to stain both ISL-1- and ISL-2-positive cells (Tsuchida et al., 1994) and has previously been used to identify the lateral ganglionic eminence in mice (Stenman et al., 2003). A monoclonal antibody against Nkx2.1 (Labvision, Fremont, CA; clone 8G7G3/1 lot 699p212) (diluted 1:100) was used to detect the region of the VZ putatively homologous to the mammalian medial ganglionic eminence. According to the manufacturer, this antibody was raised against rat TTF-1 (NKX2.1) and stains a band of molecular weight 40 kD on Western blots.

Tissue sections were placed in blocking solution containing 10% normal goat serum (Hyclone, Logan, UT), 0.25% Triton X-100 (Sigma) in PBS for 20 minutes. Tissue sections were then incubated in antibody diluted in blocking solution for 1 hour, washed 3 times in PBS, and incubated in secondary antibody for 1 hour. Alexa Fluor 555 conjugated goat antimouse (Molecular Probes) and Alexa Fluor 488 conjugated goat antirabbit (Molecular Probes) secondary antibodies were used diluted to 1:250 in blocking solution. Cy5 antirabbit (Jackson Laboratories, West Grove, PA) was used diluted to 1:100 in blocking solution.

Colabeling of antibodies and GFP was determined using confocal microscopy. In many cases antibodies could not penetrate deep enough into the tissue section to reach the depth of the cell bodies of GFP+ neurons. In these cases, since we were unable to determine whether the neuron expressed the particular antigen, we did not include those GFP+ cells in our immunohistochemical analysis.

Image acquisition and processing

Photomicrographs were obtained using a Nikon PCM2000 confocal microscope or an Olympus IX70 epifluorescence microscope and Retiga 1300 digital CCD camera (Qimaging, Surrey, BC, Canada). Neurolucida (MicroBrightField, Williston, VT) was used to trace and record the positions of new neurons and song nuclei from brain sections. Photoshop (Adobe Systems, Mountain View, CA) was used to add color, merge images, and adjust contrast and brightness. ImageJ was used to merge serial sections acquired with the confocal microscope.

RESULTS

Expression patterns of homeobox and T-box transcription factors in the ventricular zone of juvenile songbirds

To determine whether the VZs of juvenile songbirds and embryonic birds and mammals maintain similar patterns of gene expression, we examined the expression of TBR1 and members of the DLX gene family using antibodies raised against the C-terminus of TBR1 (Hsueh et al., 2000) and against a protein domain that is conserved among members of the DLX gene family (Panganiban et al., 1995). DLX-positive (DLX+) cells were present in the ventral VZ ranging from the ventral end of the ventricular wall to the border of the mesopallium–nidopallium (Fig. 1D). The highest level of expression was observed in the ventricular wall adjacent to the striatum. This region corresponds to the previously described ventral proliferative "hot spot" that contains a high number of mitotic cells and radial glia (Fig. 1C) (Alvarez-Buylla et al., 1990b; Dewulf and Bottjer, 2005). DLX+ cells were also observed in the striatum itself, in the medial pallium, and to a lesser extent in the lateral and dorsal pallium.

In the mammalian embryo the DLX-expressing region of the VZ is further divided into the LGE and the MGE. A region homologous to the mammalian LGE and MGE has also been previously described in embryonic chick brain (Puelles et al., 2000). In mice the LGE can be detected using antibodies against homeodomain-containing transcription factors ISL-1 and ISL-2 (ISL-1/2) (Stenman et al., 2003). This region is believed to be the source of the medium spiny neurons of the striatum (Deacon et al., 1994; Wichterle et al., 2001). The MGE can be identified by expression of the homeodomain-containing transcription factor NKX2.1 and is thought to be the source of cortical parvalbumin- and somatostatin-expressing interneurons (Xu et al., 2004) (Butt et al., 2005). In the DLX+ portion of the lateral ventricle in the juvenile zebra finch we observed expression of both ISL-1/2 and NKX2.1 (Fig. 1F,G), suggesting the existence of LGE-like and MGE-like progenitor zones in the postnatal songbird brain. ISL-1/2 was expressed throughout the VZ adjacent to the striatum and NKX2.1 was expressed primarily in the ventralmost portion of the lateral ventricle.

TBR1 was expressed throughout the lateral and dorsal pallium and in the adjacent VZ (Fig. 1E). The density of

The Journal of Comparative Neurology. DOI 10.1002/cne

NEUROGENESIS IN SONGBIRDS   205

TBR1 cells was highest in the hyperpallium and mesopallium, lower in the nidopallium, and lower still in the arcopallium. TBR1 expression was absent from the striatum, thalamus, hippocampus, and cerebellum. Interestingly, HVC and RA contained a higher density of cells and a greater intensity of TBR1 staining than surrounding brain regions. Cells in the lateral magnocellular nucleus of the nidopallium (LMAN) were also positive for TBR1, although the cell density and signal intensity were not obviously different from the surrounding nidopallium.

Expression of TBR1 was highest in HVC, the wall of the lateral ventricle dorsal to HVC (data not shown), and in the anterior edge of the dorsal aspect of the lateral ventricle. This latter region is rich in radial glia and corresponds anatomically to the dorsal proliferative "hot spot" previously described (Alvarez-Buylla et al., 1990b; Dewulf and Bottjer, 2005). Although the VZ dorsal to HVC contains vimentin-positive cell bodies, few vimentin-positive fibers enter HVC (Alvarez-Buylla et al., 1988b). Long-distance migration of precursors for projection neurons is thought to depend on guidance provided by the long processes of radial glia. The scarcity of vimentin-positive radial fibers through HVC suggests that neurons born in the VZ dorsal to HVC may not have the ability to distribute throughout the pallium and might instead migrate exclusively into HVC.

Fate of the cells derived from the pallial ventricular zone above HVC

Based on the pattern of TBR1 expression in the finch forebrain that we observed, we hypothesized that HVC to RA projection neurons (HVC_{RA}) might originate in the dorsal portion of the VZ. The presence of vimentin-positive cells and many TBR1+ cells contained in the VZ immediately dorsal to HVC supported a hypothesis by Goldman and Nottebohm (1983) that this region of the lateral ventricle in particular might produce HVC_{RA} neurons. To test this hypothesis we used an oncoretroviral vector carrying the gene for GFP to follow the fate of neuronal progenitors in three different regions of the VZ of three juvenile zebra finches (age 28–48 days) and in four different regions in four adult female (age 90–94 days) zebra finches that spanned the TBR1+ portion of the lateral ventricle. Viral vectors based on oncoretroviruses readily infect mitotically active cells but are unable to infect nondividing cells (Roe et al., 1993) such as neurons. Animals were sacrificed 35 days after virus injection and their brains prepared for
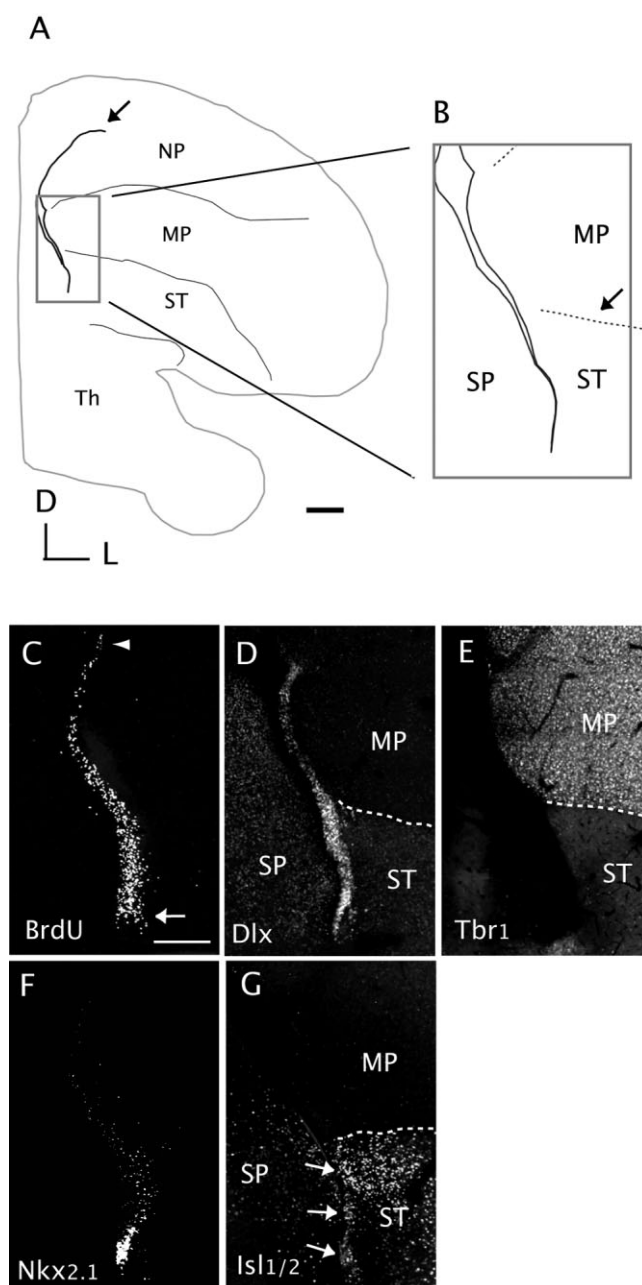

Fig. 1. Expression of homeobox and T-box transcription factors in and near the lateral ventricle of the juvenile zebra finch. **A:** Schematic diagram of the left hemisphere of the finch brain in a frontal section at the level of the anterior commissure, roughly 3.0 mm anterior of bregma. The dark line (arrow) identifies the lateral ventricle. Thin solid lines indicate the laminar divisions of the forebrain. NP, nidopallium; MP, mesopallium; ST, striatum; Th, thalamus. The box identifies the region of the lateral ventricle shown in B–E. **B:** Diagram of the region pictured in C–F. The solid black line indicates the lateral ventricle. The dotted line (arrow) represents the laminar division that separates the mesopallium (MP) from the striatum (ST). The septum (SP) lies medial to the lateral ventricle. **C:** BrdU staining in the wall of the lower region of the lateral ventricle. The highest level of cell proliferation was observed in the VZ from the border of the mesopallium (arrowhead) to the ventral tip of the lateral ventricle (arrow). This region corresponds to the ventral proliferative "hot spot" described before (Alvarez-Buylla et al., 1990b). **D:** DLX expression in the lateral ventricle and surrounding brain regions. Expression of DLX is highest in the BrdU-positive region of the lower part of the lateral ventricle. However, DLX staining was also observed in the striatum (ST), the septum (SP), and to a lesser extent in the pallium (MP). The dotted line indicates the pallial–striatal border. **E:** TBR1 is expressed exclusively in the pallium and pallial ventricular zone. The TBR1+ zone abruptly stopped at the pallial–striatal border (dotted line). **F:** Expression of NKX2.1 was primarily restricted to the ventralmost portion of the lateral ventricle. The pattern of NKX2.1 expression also overlapped with the expression of pattern of ISL-1/2, suggesting that in the juvenile finch brain the LGE-like region and MGE-like region are not completely segregated. **G:** Expression of ISL-1/2 in and around the lateral ventricle. ISL-1/2 was observed in the striatum (ST), the septum (SP), and in the lowest part of the VZ adjacent to the striatum (arrows). Dotted line indicates the pallial–striatal boarder. Scale bars = 1 mm in A; 0.5 mm in C (applies to D–G).

The Journal of Comparative Neurology. DOI 10.1002/cne

206   B.B. SCOTT AND C. LOIS

histological analysis. All seven injection sites produced many (>25) GFP+ cells with similar appearance that were found in long clusters that extended ≈200–800 μm along an axis perpendicular to the VZ at the injection site. All had round cell bodies and thin, spiny dendrites. Of these different locations, only injections into the lateral ventricle directly dorsal to HVC produced GFP+ cells in HVC. Once we determined that the VZ dorsal to HVC was a source for HVC cells, we injected three juvenile males 28–35 days posthatch with our oncoretroviral vector in this region. To confirm the identity of HVC_{RA} projection neurons, small injections of a retrograde tracer (Fluoro-Gold or cholera toxin conjugated to Alexa Fluor 555) were made into RA 4 or 7 days prior to perfusion (see Materials and Methods).

To determine the spread of infection and to identify cell types infected by our oncoretroviral vector we injected an additional three birds (males age 28–48 days posthatch) in the ventricular zone dorsal to HVC and examined the distribution of GFP-labeled cells 2–4 days later. Two days after infection GFP+ cells were observed within the VZ near the injection site and in the surrounding brain region (data not shown). Most GFP+ cells were observed within 300 μm of the injection site, and no cells were observed further than 600 μm from the injection site. These cells had round cell bodies and many appeared to have short processes oriented parallel to the ventricular wall. We inferred that these cells had undergone recent mitosis but had not yet acquired a phenotype that identified what kind of cell they would become.

Four days after infection GFP+ cells were observed in the VZ and nidopallium at distances up to 600 μm away from the injection site (Fig. 2A). At this time many cells had a morphology characteristic of migratory neurons, with a long leading process that terminated in a growth cone, a small round cell body, and a short trailing process. Interestingly, no cells with radial glia-like morphology were observed at any survival time. In addition, we never observed cells remaining in the VZ after long survival times (35 days).

Five weeks after injections targeted to the VZ above HVC, GFP+ neurons were observed in HVC and the nidopallium adjacent to HVC (Fig. 3A,B). Interestingly, no GFP+ cells remained in the VZ, nor did any GFP+ cells appear to be in the process of migration. All GFP+ cells inside HVC had a similar morphology (Fig. 3C,D). These cells had small round cell bodies between 7 and 12 μm in diameter (mean, 10.0 μm; n = 28), and thin spiny dendrites that appeared to be confined to HVC. Many GFP+ axons were visible and could be seen to exit the posterior border of HVC, project along the posterior region of the nidopallium, and enter RA, where they branched extensively. Most axons wandered in and out of the 100-μm sections. However, in one case we were able to observe an axon in its entirety projecting from HVC to RA in the same section (Fig. 4A). We observed at least two general pathways of entry into RA (Fig. 4B,C). Some axons appeared to enter RA at its most posterior aspect and branch as they entered the nucleus. Other axons appeared to arrive at the dorsal border of RA, then turn anterior and skirt the dorsal edge of the nucleus, and finally enter RA further toward its anterior tip. Interestingly, some cells appeared to bundle their axons together over the course of their projection (Fig. 4D). Even though retrograde injections covered the extent of RA, only about half (18/32) of the
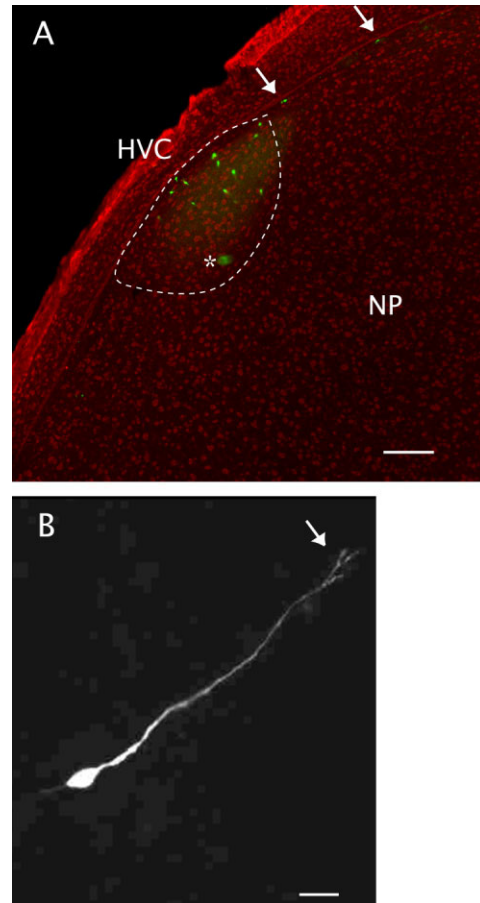

Fig. 2.   Distribution of GFP+ cells shortly after injection of retrovirus into HVC. **A:** Parasagittal section of the posterior forebrain of a bird perfused 4 days after injection of oncoretroviral vector. The section is immunostained with anti-NeuN (red) to identify the borders of HVC. Dotted line indicates the border of HVC. GFP+ cells were observed along the lateral ventricle (arrows) and within HVC. Four days after infection cells were observed up to 600 μm from the injection site. The asterisk identifies a region of autofluorescence, which was an artifact of tissue processing. NP, nidopallium. **B:** Migrating GFP+ cell derived from the DLX+ region of the lateral ventricle 7 days after injection. The cell had a short trailing process, a small cell body, and a long leading process with a growth cone at its tip (arrow). This morphology is typical of GFP+ cells observed 2–7 days after infection, and similar to that of migrating cells in the adult avian and embryonic mammalian brain. This cell was found in the wall of the lateral ventricle dorsal to the injection site with its leading process oriented dorsally toward the pallium. Scale bars = 200 μm in A; 10 μm in B.

GFP+ neurons in HVC were labeled with retrograde tracer. Previous studies have obtained similar percentages of BrdU+ cells backfilled from RA 30 days after BrdU injection, and have noted that the percentage of colabeled cells increases over time (Kirn et al., 1991, 1999). This suggests that at least a portion of our GFP+ cells in HVC that were not backfilled were somewhat immature HVC_{RA} neurons. Moreover, all GFP+ cells appeared similar in appearance to previously described HVC_{RA} cells (Mooney and Prather, 2005). These observations suggest the following, not necessarily mutually exclusive, possibilities: 1) In addition to HVC_{RA} cells, the VZ above HVC produces a
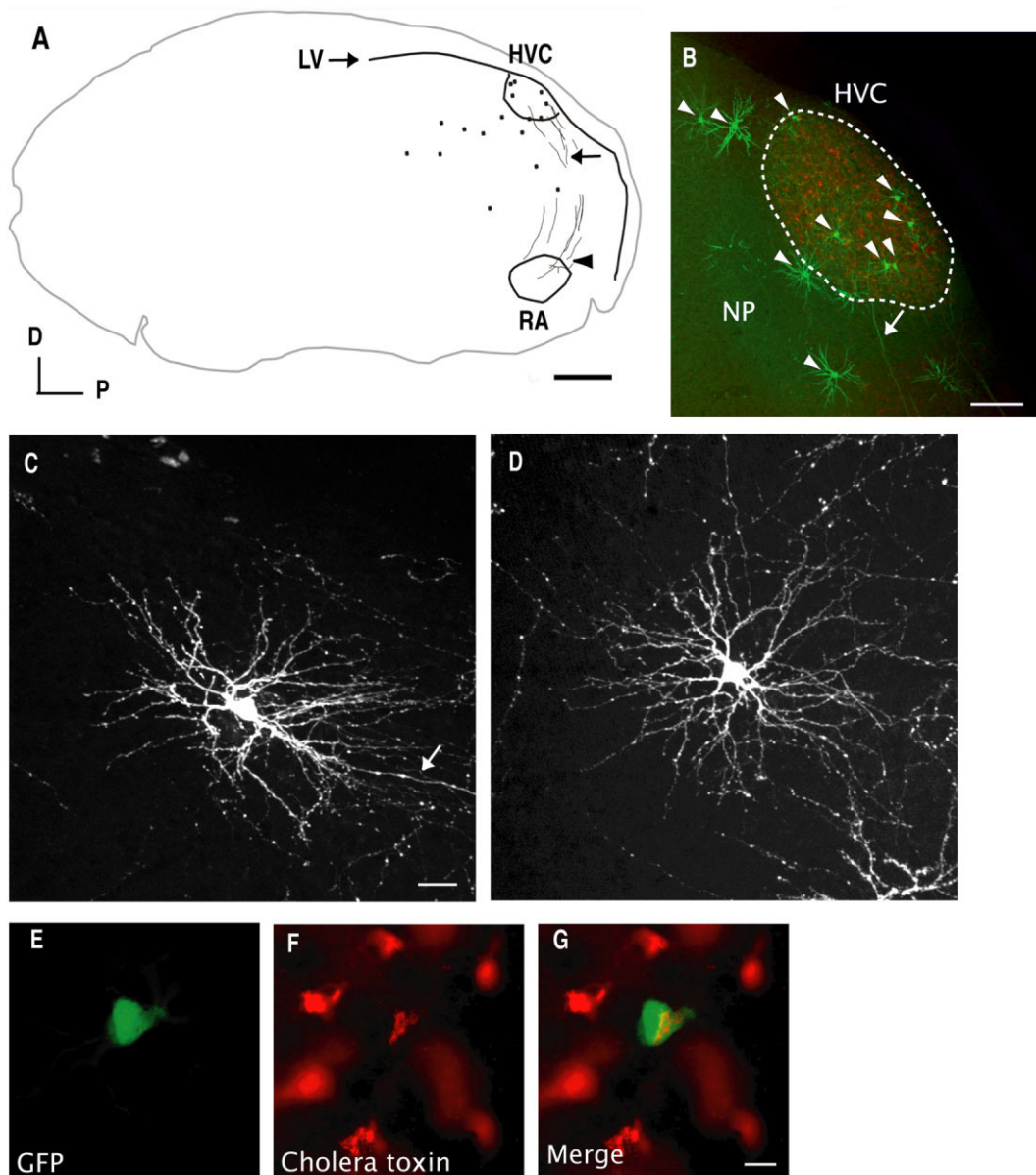
Fig. 3. Addition of new projection cells to HVC during song learning. **A:** Tracing of a parasagittal forebrain section obtained from a posthatch day 65 zebra finch 35 days after injection in the VZ dorsal to HVC. Cells (black squares) were observed in HVC and the surrounding nidopallium. Thick black lines indicate the lateral ventricle (LV) and the boundaries of HVC and RA. Axons were observed originating from HVC (arrow) and entering RA (arrowhead). **B:** GFP+ neurons (green, indicated by arrowheads) were observed in HVC and the surrounding nidopallium (NP). HVC to RA projecting neurons are labeled with a retrograde tracer injected into RA (red). GFP positive axons (arrow) can be observed exiting the posterior portion of HVC. **C:** Image of a GFP+ cell within HVC. The morphology of this cell is typical of the HVC cells that project to RA, with small round body, thin spiny dendrites, and a prominent axon (arrow). **D:** Image of a second GFP+ cell within HVC for comparison. **E–G:** GFP+ cells in HVC labeled with the retrograde tracer cholera toxin injected into RA. E: GFP+ cell. F: Alexa Fluor 555 conjugated to cholera toxin. G: Merged images of GFP and Alexa Fluor 555 conjugated to cholera toxin. Scale bars = 1 mm in A; 100 μm in B; 20 μm in C (applies to D); 10 μm in G (applies to E,F).

class of spiny interneurons that do not project to RA. 2) Some HVC$_{RA}$ neurons had not yet extended axons into RA 35 days after their birth. 3) Labeling of HVC$_{RA}$ cells with certain retrograde tracers may be partial, so that only a portion of cells with axons within RA are backfilled. Some GFP+ neurons were observed in the nidopallium outside HVC. These cells were morphologically similar to HVC$_{RA}$ cells but, in general, had thicker dendrites that were more

densely covered with spines. In addition, their axons were thin and difficult to detect and we did not characterize their projection pattern.

Fate of cells derived from the ventricular zone adjacent to the striatum

To follow the fate of cells born in the DLX+ portion of the lateral ventricle adjacent to the striatum, we injected

this area with 150–1,000 nL of oncoretroviral vector and 35 days after infection we examined the identity and position of the GFP+ cells. Although we did not attempt to thoroughly characterize the migration patterns of these cells, we examined one bird 7 days after infection. We observed cells that, based on their morphology, appeared to be in the process of migration in two directions, 1) dorsally toward the pallium along the wall of the lateral ventricle, and 2) laterally along the radial glia tracts that

run in the lamina that separates the striatum and pallium. These cells had a long leading process, whose orientation we used to infer direction of migration, with an apparent growth cone at its distal end, and a short presumed trailing process (Fig. 2B). These cells resembled migrating neuroblasts in the developing mammalian cortex. Cell migration from the subpallial VZ into the pallium has been observed before in embryonic birds and mammals (Cobos et al., 2001; Marin and Rubenstein, 2003), and is thought to take place by a distinct type of migration, called tangential migration, that occurs independent of radial glia. Five weeks after infection, no migrating GFP+ cells remained; instead, all labeled cells appeared to have a mature neuronal phenotype. Mature GFP+ cells appeared distributed throughout the hyperpallium, mesopallium, nidopallium (including HVC), and striatum (including Area X) (Fig. 5A). The furthest cell appeared more than 8 mm away from the site of injection. Few GFP+ cells were detected in the arcopallium, a brain region that has been shown to have a low rate of new neuron incorporation after hatching (Alvarez-Buylla et al., 1994).

Area X. The vast majority of the GFP+ cells in the striatum had a morphology that was distinct from the cells observed in HVC. Labeled cells in Area X had highly branched dendritic arbors and an axon that appeared confined to Area X. The soma of GFP-labeled cells in Area X was between 6 and 10 μm in diameter (mean, 7.7 μm; n = 49), and their dendrites were densely covered with spines (Fig. 5C–E). These cells bore close resemblance to the previously characterized spiny neurons of Area X (Farries and Perkel, 2002) and to the medium spiny neurons of the mammalian striatum (Wilson, 2004). To further characterize this cell population we performed immunohistochemistry against DARPP-32 (Fig. 5F–H), a specific marker for medium spiny neurons in the mammalian and avian striatum (Anderson and Reiner, 1991; Reiner et al., 1998). The DARPP-32 antibody did not penetrate deeply into our vibratome sections and therefore we were only able to characterize seven GFP+ cells in the superficial region of our sections. Six of these seven cells were also positive for DARPP-32.

HVC. GFP+ cells were also detected throughout the pallium including HVC and HVC shelf (Figs. 6D, 7D). The number of new neurons that were detected in HVC after viral injection in the lower region of the VZ was relatively low (16 neurons from four injected hemispheres). It is important to notice that HVC occupies only a very small percentage of the volume of the forebrain and perhaps,
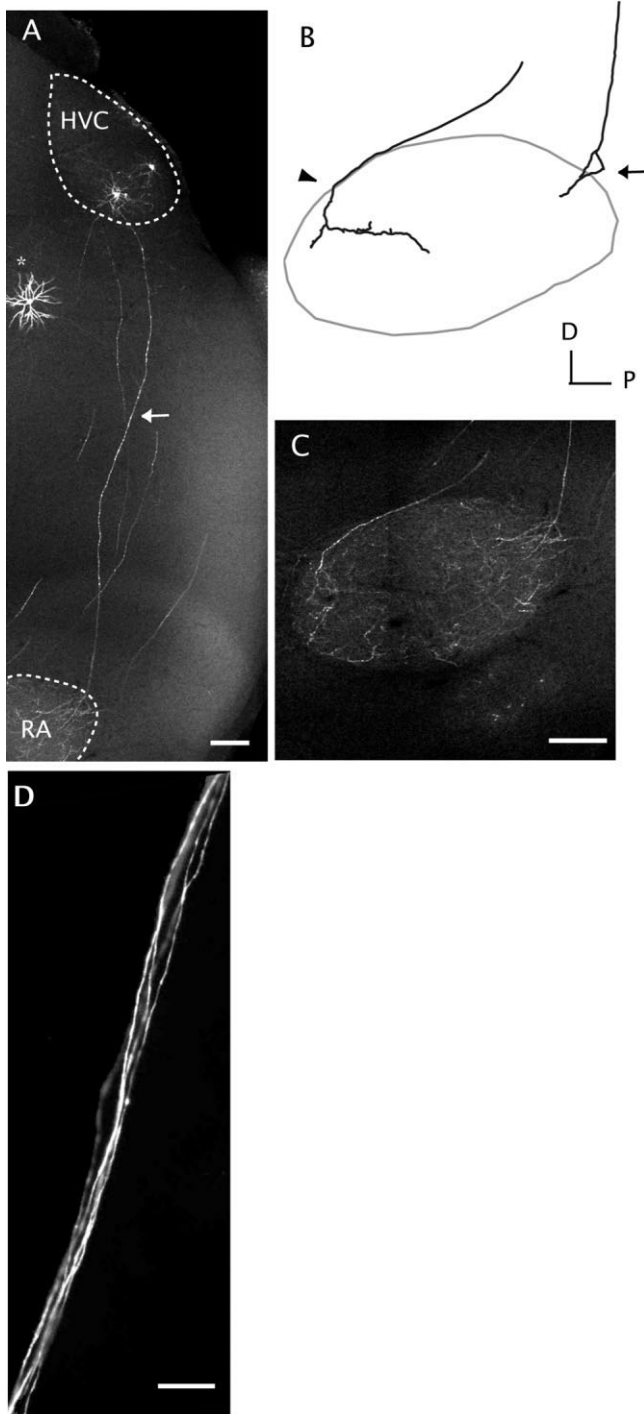

Fig. 4. Characterization of HVC projection cells born during vocal learning. **A:** GFP-labeled cells in HVC and the surrounding nidopallium following infection of the VZ dorsal to HVC. GFP+ axon (arrow) from HVC to RA observed in its entirety. A GFP-labeled cell outside of HVC is labeled with an asterisk. **B:** Tracing of the innervation of RA by axons of HVC projection cells. Two patterns of innervation were observed. Some axons, such as the one pictured in A, entered RA at the posterior end of the nucleus (arrow). Other axons appeared to skirt the dorsal edge of RA and enter the nucleus at the anterior edge (arrowhead). In either case the axon of the HVC projection cell ramified immediately upon entry into RA sending out at least two collaterals that branched extensively throughout the nucleus. **C:** Photograph of the innervation of RA used to produce the tracing in B. **D:** Axon bundles in the HVC to RA projection. Scale bars = 250 μm in A; 200 μm in C; 10 μm in D.
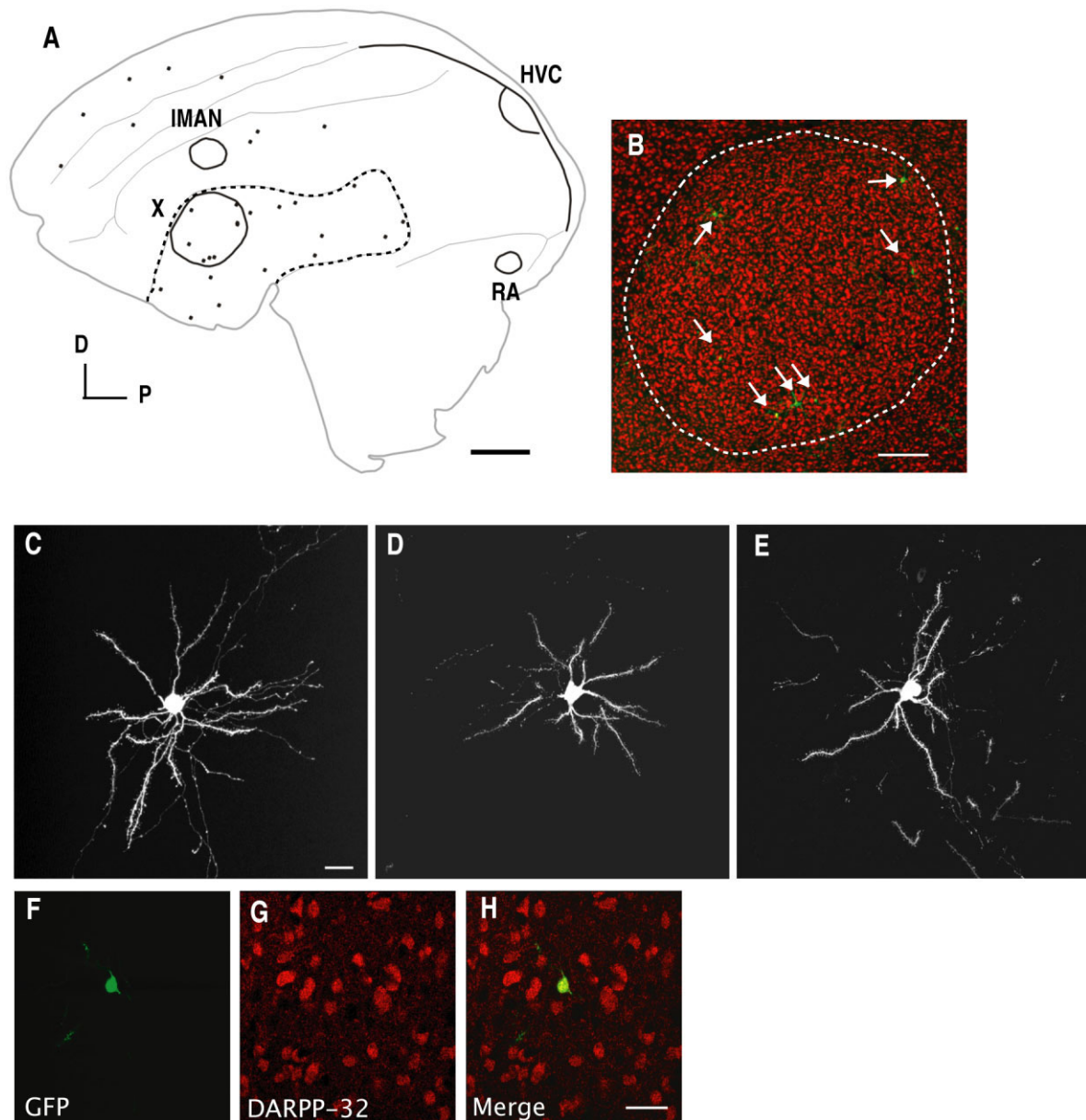
Fig. 5. Neuron addition in Area X. **A:** Tracing of the distribution of GFP+ cells in a parasagittal section of the zebra finch forebrain 35 days after infection of the ventral VZ with retroviruses. Cells (black squares) could be observed throughout the striatum, including Area X and pallium (dotted line indicates the border of the striatum and pallium). New neurons were also detected in HVC, although not in this section. **B:** GFP+ cells (green, indicated by arrows) in Area X immunostained with an antibody against NeuN (red). Dotted line indicated the border of Area X. **C–E:** Confocal microscopy images of GFP+ cell in Area X (C,D) and surrounding striatum (E) 35 days after infection of the avian MGE and LGE. The morphology of these cells is characteristic of GFP+ cells in Area X and the surrounding striatum. These cells had small cell bodies and thick spiny dendrites. (F-H) GFP+ cells in Area X express DARPP3-32. **F:** GFP cell body in Area X imaged with confocal microscope. **G:** DARPP-32 immunostaining in the same optical section as D. **H:** Merged images of GFP and DARPP-32 immunostaining. Scale bars = 1 mm in A; 200 μm in B; 10 μm in C (applies to D,E); 25 μm in H (applies to F,G).

accordingly, it may only receive a small percentage of the neurons produced in this area of the VZ. In addition, the low number of GFP+ cells observed following injection of the DLX-expressing region of the VZ could reflect a low rate of interneuron addition in HVC at the age our birds were injected. We observed at least two distinct cell morphologies in HVC and HVC shelf. The first cell type observed (9/16) had an oblong cell body of about 9 by 14 μm

in size, a large dendritic tree with few primary dendrites, and an axon that appeared confined to HVC. The dendrites were thicker than those of the HVC_{RA} projection cells and they were densely covered with large spines (Fig. 6A–C). This cell type resembles previously characterized neurons in the canary HVC identified by horseradish peroxidase (HRP) filling of neurons (Paton and Nottebohm, 1984) and by Golgi stain (Nixdorf et al., 1989). Immuno-
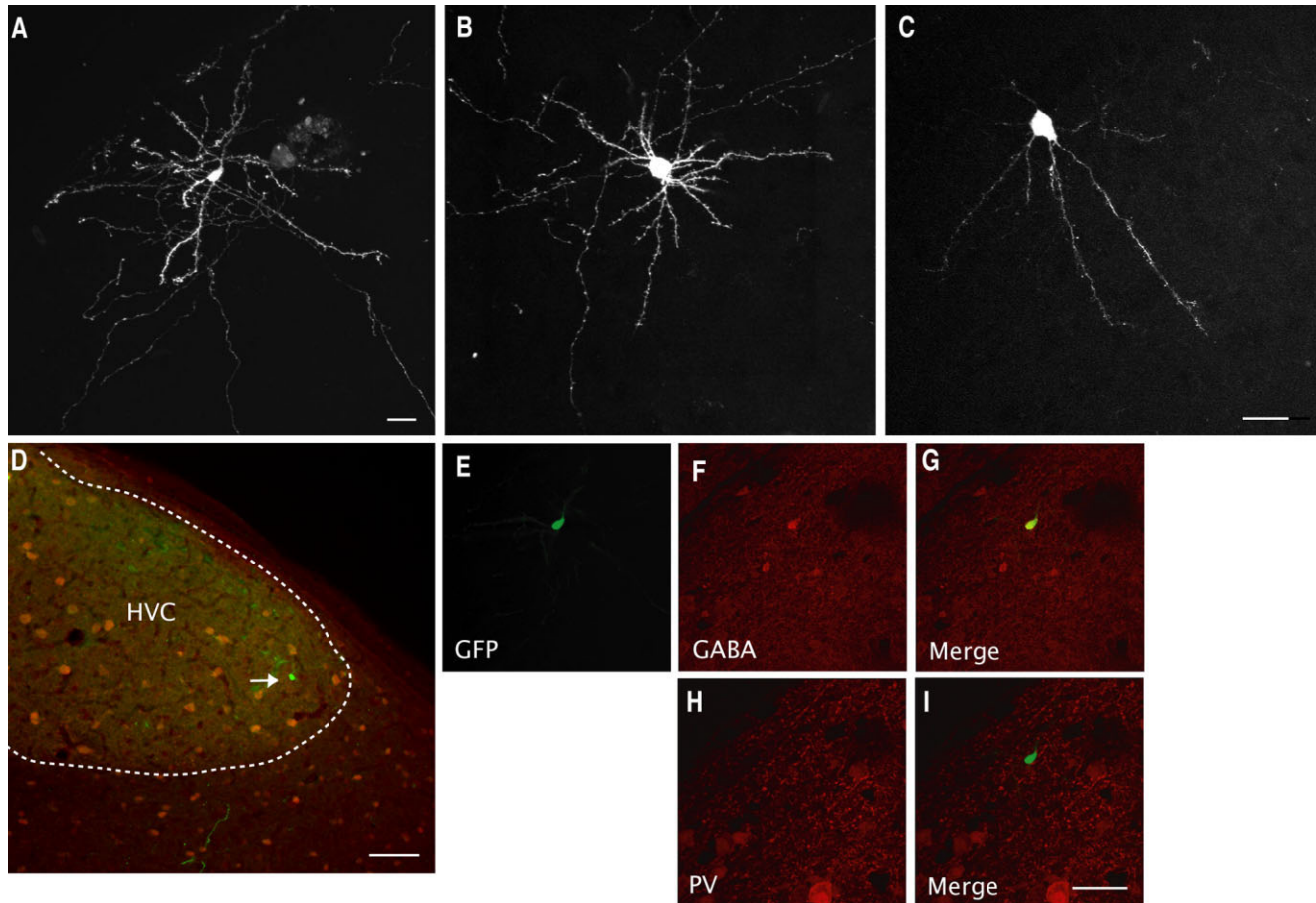
The Journal of Comparative Neurology. DOI 10.1002/cne

210   B.B. SCOTT AND C. LOIS

Fig. 6. Newly generated spiny interneuron in HVC. **A–C:** Three examples of new spiny interneurons in HVC born in the ventral ventricular zone. These cells were characterized by their small oblong cell bodies and thick spiny dendrites. **D:** GFP+ cell (green, indicated by arrow) observed in a parasagittal section containing HVC. Immunohistochemistry against parvalbumin (red) is used to identify the boundary of HVC. Dotted line indicates the border of HVC.

E–I: Immunohistochemical analysis of spiny interneurons in HVC using confocal microscopy. E: GFP+ cell body in HVC. F: GABA immunostaining. G: Merged images of GFP and GABA-immunostaining. H: PV staining of the same region. I: Merged images of GFP and PV immunostaining. Scale bars = 20 μm in A,C (applies to B); 100 μm in D; 50 μm in I (applies to E–H).

staining of these GFP+ cells revealed that they were positive for GABA and negative for the calcium-binding protein parvalbumin (PV) (Fig. 6E–I). In some cases parvalbumin-positive (PV+) processes appeared to surround the cell bodies of these neurons (Fig. 7H). The pattern of parvalbumin staining appeared identical to the previously described staining pattern in HVC (Wild et al., 2005).

We observed a second neuron type in HVC and the surrounding nidopallium with large round cell bodies, between 11 and 17μm in diameter, and large dendritic arbors (Fig. 7A–C). The dendrites of these cells were either aspiny or sparsely covered with thin spines or filopodia. We observed this cell type less frequently (4/16). We were able to characterize three out of these four cells by immunohistochemistry. All three neurons were immunopositive for GABA, and two expressed PV (Fig. 7E–J). These cells were similar to the fast-spiking PV+ inhibitory neurons in the zebra finch HVC (Mooney and Prather, 2005), as well as the PV+ inhibitory basket cells found in mammalian hippocampus (Somogyi and Klausberger, 2005) and cortex (Kawaguchi and Kubota, 1996).

Three cells (3/16) could not be easily assigned to either category. By some estimates, the number of cell types in the mammalian cortex and hippocampus is extremely large (Markram et al., 2004) and often neurons are difficult to assign to a particular type (Parra et al., 1998). The cell type composition of HVC may be as diverse as the mammalian cortex, and the unassigned cell types we observed could reflect the diversity of HVC interneurons. Alternatively, our inability to assign some neurons to a particular class may be a consequence of our histological analysis. In this study, tissue sections were cut thin (30 μm) to allow better immunohistochemical analysis. For some cells (n = 2), however, the tissue sections were too thin to adequately characterize their dendritic morphology. Future experiments labeling greater numbers of HVC interneurons will be necessary to address these uncertainties about the number of different interneuron subtypes in HVC. Our method, based on fate mapping by oncoretroviral vectors, is likely to be biased for the detection of different cell types and there may be yet additional cell classes added to the song circuit during vocal learning.
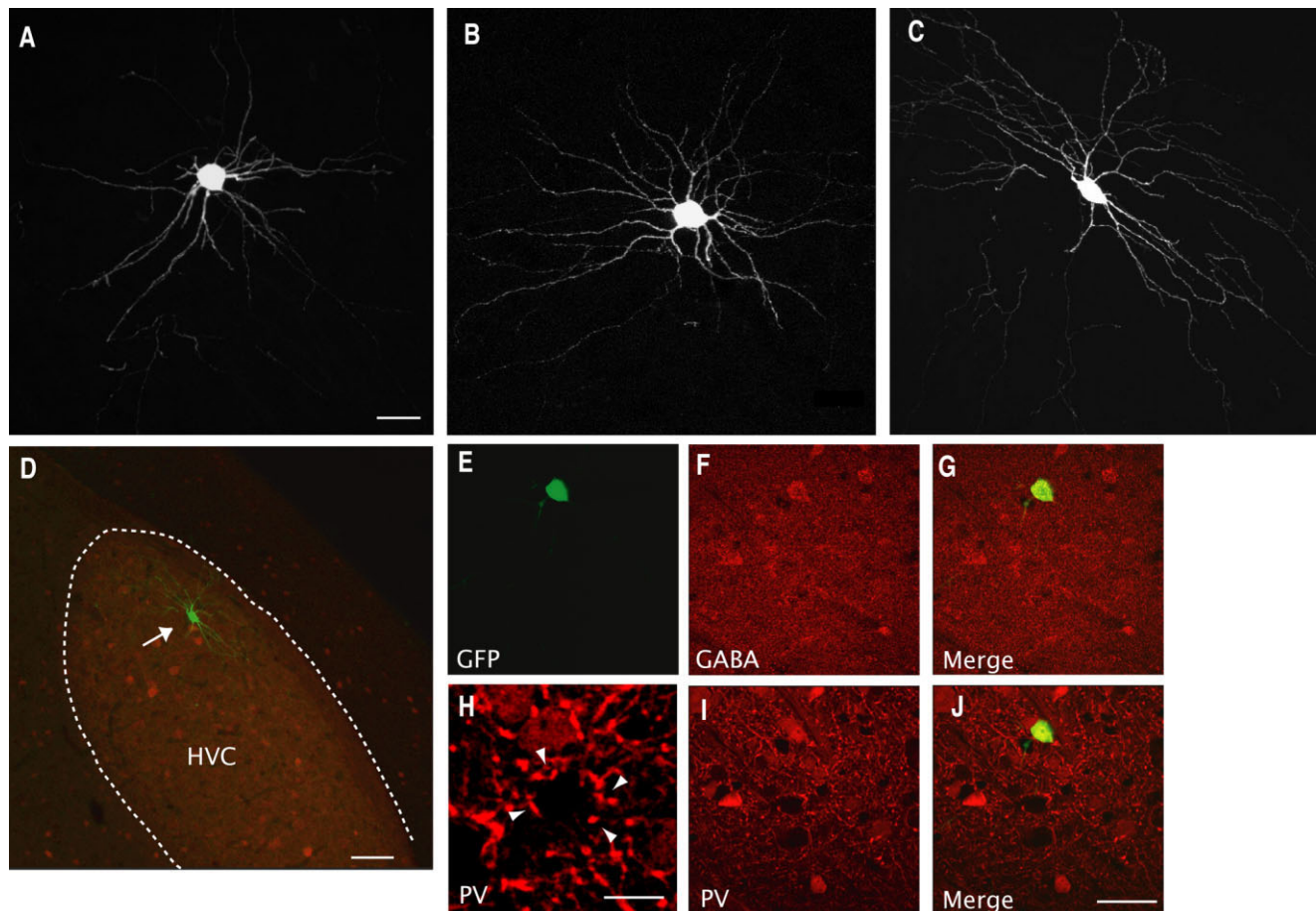
The Journal of Comparative Neurology. DOI 10.1002/cne

NEUROGENESIS IN SONGBIRDS

211

Fig. 7. Newly generated aspiny interneuron in HVC. **A–C:** Confocal microscopy images of three aspiny interneurons in HVC originating from the ventral ventricular zone. These cells were characterized by their large cell bodies and aspiny dendrites. **D:** GFP+ aspiny interneuron (arrow) in a parasagittal section of HVC. Immunohistochemistry against parvalbumin (red) is used to identify the boundary of HVC. Dotted line indicates the border of HVC. Although aspiny interneurons in HVC typically express parvalbumin, this particular cell did not. This cell is pictured at higher magnification in C. **E–J:** Immunohistochemical analysis of aspiny interneurons. E: GFP+ cell body in HVC. F: GABA immunostaining. G: Merged images of GFP and GABA-immunostaining. H: High-magnification image of parvalbumin staining. Parvalbumin was detected in cell bodies and neuropil in HVC. Parvalbumin staining revealed many varicosities (arrowheads) that often appeared to surround spherical PV− zones. These zones are probably the cell bodies of other neurons, since we sometimes observed GFP+ cell bodies surrounded by PV+ varicosities. I: Parvalbumin staining of the same region shown in C–E. J: Merged images of GFP and parvalbumin immunostaining. Scale bars = 20 μm in A (applies to B,C); 50 μm in D; 30 μm in J (applies to E–G,I; 15 μm in H).

DISCUSSION

Although the avian and mammalian forebrains differ at the level of gross morphology, several lines of evidence suggest that the basic cell types, and perhaps circuitry, are conserved between birds and mammals. Our results suggest that postnatal neurogenesis in the songbird shares some important similarities to embryonic neurogenesis in birds and mammals. Based on the expression of the transcription factors TBR1, DLX, NKX2.1, and ISL-1/2, it appears that the same pattern of gene expression present in the lateral ventricle of embryonic mice and chicks (Puelles et al., 2000; Stenman et al., 2003) persists in the brains of juvenile zebra finches. Moreover, we have demonstrated that in juvenile zebra finches these regions of the lateral ventricle produce similar neuronal subtypes to those generated from homologous regions of the embryonic mouse (Marin and Rubenstein, 2003; Xu et al., 2004; Butt et al., 2005). We observed the addition of at least four

different classes of new neurons to the song system of the juvenile zebra finch: 1) HVC to RA projection cells, 2) spiny, PV−, GABA+ neurons in HVC, 3) aspiny PV+, GABA+ neurons in HVC, and 4) medium spiny neurons in Area X, two of which, medium spiny neurons and PV+ inhibitory interneurons, have clear homologs in the mammalian forebrain.

Identity of cells targeted by oncoretroviral vectors

Oncoretroviral vectors are capable of infecting mitotically active cells, therefore it is somewhat surprising that we did not observe any GFP+ radial glia in the injection site, since these cells are know to be actively dividing stem cells that give rise to new neurons in the vertebrate forebrain (Alvarez-Buylla et al., 1990b; Noctor et al., 2001). Moreover, we did not observe any GFP+ cells remaining in the VZ after long (35 days) survival times. These obser-

The Journal of Comparative Neurology. DOI 10.1002/cne

212   B.B. SCOTT AND C. LOIS

vations suggest that we are not infecting the true stem cells that reside in the VZ, and instead are infecting either a progenitor that gives rise to migrating neuroblasts or the neuroblasts themselves during mitosis. Similar observations have been made following oncoretroviral injections into the subventricular zone of newborn mice, where the oncoretrovirus appears to infect newborn cells that migrate to the olfactory bulb, but not the stem cells within the walls of the lateral ventricle (Luskin, 1993).

Origin of HVC$_{RA}$ projection neurons

Previous studies using a combination of retrograde tracing from RA and ^{3}H thymidine labeling identified the majority of HVC neurons born after hatching as HVC$_{RA}$ neurons (Nordeen and Nordeen, 1988; Alvarez-Buylla et al., 1988a, 1990a). Our results confirm the addition of HVC$_{RA}$ neurons into the juvenile finch brain and identify the VZ above HVC as their site of origin, as suggested by Goldman and Nottebohm (1983). Our data suggest that the VZ above HVC is the only region of the VZ that generates HVC$_{RA}$ neurons during vocal learning. However, this region of the V2 may also produce other types of neurons exclusively for HVC, as there were, after all injections; GFP+ cells in the nearby nidopallium.

Since the juvenile zebra finch VZ above HVC appears to generate HVC$_{RA}$ projection neurons, but not neurons that project to Area X or interneurons, it should be possible to specifically target this cell type by infection of the precursor cells with an oncoretroviral vector. In this study we introduced GFP into a subset of HVC$_{RA}$ neurons. However, oncoretroviral vectors can be engineered to carry an expression cassette containing any gene of interest. Genes of interest can also be introduced into fully mature HVC$_{RA}$ neurons by direct infection of HVC with lentiviral-based vectors (B.B.S., unpubl. obs.), a class of vectors that can infect both postmitotic cells as well as cells that are actively proliferating (Naldini et al., 1996). However, this method would also target other neuronal cell types in HVC, such as interneurons and HVC to Area X projection cell, as well as nonneuronal cell types, such as astrocytes.

Origin of HVC GABAergic interneurons

Our results also identify the site of interneuron origin for HVC. Following oncoretroviral injections into the ventral VZ we observed at least two classes of GABAergic interneurons in HVC. These cells may migrate to their destination in the song circuit by tangential migration, a form of migration independent of radial glia used by interneuron precursors in the mammalian forebrain (Anderson et al., 1997).

Of the two classes of new HVC interneurons we observed, the addition of PV+ aspiny cells is particularly interesting. These cells resemble the fast-spiking PV+ basket cells of the mammalian cortex and hippocampus in terms of morphology, electrophysiology, immunohistochemistry, and developmental origin. In mammals, fast-spiking basket cells are thought to contribute to precise spike timing (Pouille and Scanziani, 2001). PV+ aspiny cells in HVC have been shown to mediate fast feedforward inhibition onto projection neurons and interneurons (Mooney and Prather, 2005). The firing patterns of interneurons and projection neurons of the song system during song-related activity have submillisecond temporal precision (Yu and Margoliash, 1996; Chi and Margoliash, 2001; Hahnloser et al., 2002), and perhaps PV+ aspiny cells in

HVC contribute to the precision of this timing. PV+ basket cells have also been implicated in the control of the critical period of ocular dominance plasticity in the mammalian visual cortex (Hensch, 2005). It would be of considerable interest if the addition of PV+ interneurons into the juvenile brain had a similar role in the sensitive period for vocal learning.

It is more difficult to speculate on the function of the spiny, PV−, GABAergic interneurons in HVC because their electrophysiology has not been characterized.

Nature and role of the new Area X neurons

Postnatal new neuron addition occurs in songbirds at its highest rate in Area X and the surrounding striatum (Alvarez-Buylla et al., 1994). We were able to identify these new cells as medium spiny neurons (MSNs), the principal neurons of the vertebrate striatum. This result is somewhat surprising. While the circuitry and cell type composition of the basal ganglia appears conserved between mammals and birds (Doupe et al., 2005), MSNs were only recently identified in avian striatum (Farries and Perkel, 2000). MSNs are a major component of the mammalian basal ganglia and have attracted a great deal of interest because these cells are preferentially lost in Huntington's disease (Mitchell et al., 1999).

The addition of MSNs may be related to vocal learning. Area X is the input structure to the anterior forebrain pathway (AFP), a neural pathway essential for song learning, but not for the production of learned song (Bottjer et al., 1984). MSNs are thought to be the primary input cells in Area X, and therefore the AFP, receiving direct synaptic input from both HVC and LMAN (Farries et al., 2005). The AFP has been hypothesized to control the variability of the juvenile song and may provide a means for songbirds to explore a range of vocalizations (Kao et al., 2005; Olveczky et al., 2005); however, the precise function of Area X in song learning has been difficult to determine. One intriguing hypothesis is that Area X may be involved in the acquisition of the tutor's song (Ding and Perkel, 2004; Singh et al., 2005). Perhaps new medium spiny neurons are involved in the formation of new auditory memories that are used to shape the output of the AFP during singing (Solis and Doupe, 2000).

Comparative neuroanatomy based on cell type

Historically, comparative vertebrate neuroanatomy has focused on the homologies between similar brain regions found in different vertebrate species (Nieuwenhuys et al., 1998). However, evidence from fate mapping experiments and mouse mutants has shown that a single forebrain region is composed of a variety of cells types, each derived from a distinct lineage (Marin and Rubenstein, 2003). Moreover, it has been observed that anatomically distinct brain regions, such as the striatum, neocortex, amygdala, and hippocampus, contain neurons, particularly interneurons, that share the same developmental origin (Marin et al., 2000; Reid and Walsh, 2002; Nery et al., 2002; Xu et al., 2004) and have very similar physiological properties. Since cell types appear to be shared across anatomically distinct brain areas within a species and across similar brain areas in different vertebrate species, it seems important to consider the cell type as a conserved unit that may have similar functions in different neural circuits.

Our experiments provide evidence that cells in the vocal learning circuit of the avian forebrain share a strong homology to cell types found in the mammalian cortex and basal ganglia. Previous studies have suggested the existence of similar cell types in the avian and mammalian forebrain based on morphological, electrophysiological, and immunohistochemical evidence (Wild et al., 1993; Farries and Perkel, 2000; Mooney and Prather, 2005). Based on similarities of cell connectivity, it has been hypothesized that although the avian and mammalian forebrains differ at the level of gross anatomy, they share equivalent circuits (Karten, 1997; Jarvis et al., 2005). We propose that different cell types in the vertebrate brain may have evolved to perform certain computations in a neural circuit, and that a particular cell type can be used in different brain regions where its specialized function is needed. Taking a comparative approach across different taxa may help to identify the function of specific cell types of the forebrain. The existence of specialized brain circuits for learning a robust quantifiable behavior makes the nervous system of songbirds a particularly attractive system for exploring the functional contribution of different neuronal types.

LITERATURE CITED

Alvarez-Buylla A, Nottebohm F. 1988. Migration of young neurons in adult avian brain. Nature 335:353–354.

Alvarez-Buylla A, Theelen M, Nottebohm F. 1988a. Birth of projection neurons in the higher vocal center of the canary forebrain before, during, and after song learning. Proc Natl Acad Sci U S A 85:8722–8726.

Alvarez-Buylla A, Theelen M, Nottebohm F. 1988b. Mapping of radial glia and of a new cell type in adult canary brain. J Neurosci 8:2707–2712.

Alvarez-Buylla A, Kirn JR, Nottebohm F. 1990a. Birth of projection neurons in adult avian brain may be related to perceptual or motor learning. Science 249:1444–1446.

Alvarez-Buylla A, Theelen M, Nottebohm F. 1990b. Proliferation "hot spots" in adult avian ventricular zone reveal radial cell division. Neuron 5:101–109.

Alvarez-Buylla A, Ling CY, Yu WS. 1994. Contribution of neurons born during embryonic, juvenile, and adult life to the brain of adult canaries: regional specificity and delayed birth of neurons in the song-control nuclei. J Comp Neurol 347:233–248.

Alvarez-Buylla A, Garcia-Verdugo JM, Mateo AS, Merchant-Larios H. 1998. Primary neural precursors and intermitotic nuclear migration in the ventricular zone of adult canaries. J Neurosci 18:1020–1037.

Anderson KD, Reiner A. 1991. Immunohistochemical localization of DARPP-32 in striatal projection neurons and striatal interneurons: implications for the localization of D1-like dopamine receptors on different types of striatal neurons. Brain Res 568:235–243.

Anderson SA, Eisenstat DD, Shi L, Rubenstein JL. 1997. Interneuron migration from basal forebrain to neocortex: dependence on Dlx genes. Science 278:474–476.

Bottjer SW, Miesner EA, Arnold AP. 1984. Forebrain lesions disrupt development but not maintenance of song in passerine birds. Science 224:901–903.

Brown ST, Wang J, Groves AK. 2005. Dlx gene expression during chick inner ear development. J Comp Neurol 483:48–65.

Butt SJ, Fuccillo M, Nery S, Noctor S, Kriegstein A, Corbin JG, Fishell G. 2005. The temporal and spatial origins of cortical interneurons predict their physiological subtype. Neuron 48:591–604.

Chi Z, Margoliash D. 2001. Temporal precision and temporal drift in brain and behavior of zebra finch song. Neuron 32:899–910.

Cobos I, Puelles L, Martinez S. 2001. The avian telencephalic subpallium originates inhibitory neurons that invade tangentially the pallium (dorsal ventricular ridge and cortical areas). Dev Biol 239:30–45.

Deacon TW, Pakzaban P, Isacson O. 1994. The lateral ganglionic eminence is the origin of cells committed to striatal phenotypes: neural transplantation and developmental evidence. Brain Res 668:211–219.

Dewulf V, Bottjer SW. 2005. Neurogenesis within the juvenile zebra finch telencephalic ventricular zone: a map of proliferative activity. J Comp Neurol 481:70–83.

Ding L, Perkel DJ. 2004. Long-term potentiation in an avian basal ganglia nucleus essential for vocal learning. J Neurosci 24:488–494.

Doupe AJ, Perkel DJ, Reiner A, Stern EA. 2005. Birdbrains could teach basal ganglia research a new song. Trends Neurosci 28:353–363.

Farries MA, Perkel DJ. 2000. Electrophysiological properties of avian basal ganglia neurons recorded in vitro. J Neurophysiol 84:2502–2513.

Farries MA, Perkel DJ. 2002. A telencephalic nucleus essential for song learning contains neurons with physiological characteristics of both striatum and globus pallidus. J Neurosci 22:3776–3787.

Farries MA, Ding L, Perkel DJ. 2005. Evidence for "direct" and "indirect" pathways through the song system basal ganglia. J Comp Neurol 484:93–104.

Goldman SA, Nottebohm F. 1983. Neuronal production, migration, and differentiation in a vocal control nucleus of the adult female canary brain. Proc Natl Acad Sci U S A 80:2390–2394.

Hahnloser RH, Kozhevnikov AA, Fee MS. 2002. An ultra-sparse code underlies the generation of neural sequences in a songbird. Nature 419:65–70.

Hemmings HC Jr, Greengard P. 1986. DARPP-32, a dopamine- and adenosine 3′:5′-monophosphate-regulated phosphoprotein: regional, tissue, and phylogenetic distribution. J Neurosci 6:1469–1481.

Hensch TK. 2005. Critical period plasticity in local cortical circuits. Nat Rev Neurosci 6:877–888.

Hevner RF, Hodge RD, Daza RA, Englund C. 2006. Transcription factors in glutamatergic neurogenesis: conserved programs in neocortex, cerebellum, and adult hippocampus. Neurosci Res 55:223–233.

Hsueh YP, Wang TF, Yang FC, Sheng M. 2000. Nuclear translocation and transcription regulation by the membrane-associated guanylate kinase CASK/LIN-2. Nature 404:298–302.

Jarvis ED, Gunturkun O, Bruce L, Csillag A, Karten H, Kuenzel W, Medina L, Paxinos G, Perkel DJ, Shimizu T, Striedter G, Wild JM, Ball GF, Dugas-Ford J, Durand SE, Hough GE, Husband S, Kubikova L, Lee DW, Mello CV, Powers A, Siang C, Smulders TV, Wada K, White SA, Yamamoto K, Yu J, Reiner A, Butler AB. 2005. Avian brains and a new understanding of vertebrate brain evolution. Nat Rev Neurosci 6:151–159.

Kao MH, Doupe AJ, Brainard MS. 2005. Contributions of an avian basal ganglia-forebrain circuit to real-time modulation of song. Nature 433:638–643.

Karten HJ. 1997. Evolutionary developmental biology meets the brain: the origins of mammalian cortex. Proc Natl Acad Sci U S A 94:2800–2804.

Kawaguchi Y, Kubota Y. 1996. Physiological and morphological identification of somatostatin- or vasoactive intestinal polypeptide-containing cells among GABAergic cell subtypes in rat frontal cortex. J Neurosci 16:2701–2715.

Kirn JR, Alvarez-Buylla A, Nottebohm F. 1991. Production and survival of projection neurons in a forebrain vocal center of adult male canaries. J Neurosci 11:1756–1762.

Kirn JR, Fishman Y, Sasportas K, Alvarez-Buylla A, Nottebohm F. 1999. Fate of new neurons in adult canary high vocal center during the first 30 days after their formation. J Comp Neurol 411:487–494.

Lois C, Hong EJ, Pease S, Brown EJ, Baltimore D. 2002. Germline transmission and tissue-specific expression of transgenes delivered by lentiviral vectors. Science 295:868–872.

Luskin MB. 1993. Restricted proliferation and migration of postnatally generated neurons derived from the forebrain subventricular zone. Neuron 11:173–189.

Marin O, Rubenstein JL. 2003. Cell migration in the forebrain. Annu Rev Neurosci 26:441–483.

Marin O, Anderson SA, Rubenstein JL. 2000. Origin and molecular specification of striatal interneurons. J Neurosci 20:6063–6076.

Markram H, Toledo-Rodriguez M, Wang Y, Gupta A, Silberberg G, Wu C. 2004. Interneurons of the neocortical inhibitory system. Nat Rev Neurosci 5:793–807.

Mitchell IJ, Cooper AJ, Griffiths MR. 1999. The selective vulnerability of striatopallidal neurons. Prog Neurobiol 59:691–719.

Mooney R, Prather JF. 2005. The HVC microcircuit: the synaptic basis for interactions between song motor and vocal plasticity pathways. J Neurosci 25:1952–1964.

Naldini L, Blomer U, Gallay P, Ory D, Mulligan R, Gage FH, Verma IM, Trono D. 1996. In vivo gene delivery and stable transduction of nondividing cells by a lentiviral vector. Science 272:263–267.

The Journal of Comparative Neurology. DOI 10.1002/cne

214

B.B. SCOTT AND C. LOIS

Nery S, Fishell G, Corbin JG. 2002. The caudal ganglionic eminence is a source of distinct cortical and subcortical cell populations. Nat Neurosci 5:1279–1287.

Nieuwenhuys R, Donkelaar HJt, Nicholson C. 1998. The central nervous system of vertebrates. Berlin: Springer.

Nixdorf BE, Davis SS, DeVoogd TJ. 1989. Morphology of Golgi-impregnated neurons in hyperstriatum ventralis, pars caudalis in adult male and female canaries. J Comp Neurol 284:337–349.

Noctor SC, Flint AC, Weissman TA, Dammerman RS, Kriegstein AR. 2001. Neurons derived from radial glial cells establish radial units in neocortex. Nature 409:714–720.

Nordeen KW, Nordeen EJ. 1988. Projection neurons within a vocal motor pathway are born during song learning in zebra finches. Nature 334:149–151.

Nordeen EJ, Nordeen KW. 1990. Neurogenesis and sensitive periods in avian song learning. Trends Neurosci 13:31–36.

Nottebohm F. 1999. The anatomy and timing of vocal learning in birds. In: Hauser MD, Konishi M, editors. The design of animal communication. Cambridge, MA: MIT Press. p 63–110.

Nottebohm F. 2002. Why are some neurons replaced in adult brain? J Neurosci 22:624–628.

Nottebohm F. 2004. The road we travelled: discovery, choreography, and significance of brain replaceable neurons. Ann N Y Acad Sci 1016:628–658.

Olveczky BP, Andalman AS, Fee MS. 2005. Vocal experimentation in the juvenile songbird requires a basal ganglia circuit. PLoS Biol 3:e153.

Panganiban G, Sebring A, Nagy L, Carroll S. 1995. The development of crustacean limbs and the evolution of arthropods. Science 270:1363–1366.

Parra P, Gulyas AI, Miles R. 1998. How many subtypes of inhibitory cells in the hippocampus? Neuron 20:983–993.

Paton JA, Nottebohm FN. 1984. Neurons generated in the adult brain are recruited into functional circuits. Science 225:1046–1048.

Pouille F, Scanziani M. 2001. Enforcement of temporal fidelity in pyramidal cells by somatic feed-forward inhibition. Science 293:1159–1163.

Puelles L, Kuwana E, Puelles E, Bulfone A, Shimamura K, Keleher J, Smiga S, Rubenstein JL. 2000. Pallial and subpallial derivatives in the embryonic chick and mouse telencephalon, traced by the expression of the genes Dlx-2, Emx-1, Nkx-2.1, Pax-6, and Tbr-1. J Comp Neurol 424:409–438.

Reid CB, Walsh CA. 2002. Evidence of common progenitors and patterns of dispersion in rat striatum and cerebral cortex. J Neurosci 22:4002–4014.

Reiner A, Perera M, Paullus R, Medina L. 1998. Immunohistochemical localization of DARPP32 in striatal projection neurons and striatal interneurons in pigeons. J Chem Neuroanat 16:17–33.

Roe T, Reynolds TC, Yu G, Brown PO. 1993. Integration of murine leukemia virus DNA depends on mitosis. EMBO J 12:2099–2108.

Singh TD, Nordeen EJ, Nordeen KW. 2005. Song tutoring triggers CaMKII phosphorylation within a specialized portion of the avian basal ganglia. J Neurobiol 65:179–191.

Sohrabji F, Nordeen EJ, Nordeen KW. 1993. Characterization of neurons born and incorporated into a vocal control nucleus during avian song learning. Brain Res 620:335–338.

Solis MM, Doupe AJ. 2000. Compromised neural selectivity for song in birds with impaired sensorimotor learning. Neuron 25:109–121.

Somogyi P, Klausberger T. 2005. Defined types of cortical interneurone structure space and spike timing in the hippocampus. J Physiol 562:9–26.

Stenman J, Toresson H, Campbell K. 2003. Identification of two distinct progenitor populations in the lateral ganglionic eminence: implications for striatal and olfactory bulb neurogenesis. J Neurosci 23:167–174.

Stokes TM, Leonard CM, Nottebohm F. 1974. The telencephalon, diencephalon, and mesencephalon of the canary, *Serinus canaria,* in stereotaxic coordinates. J Comp Neurol 156:337–374.

Tsuchida T, Ensini M, Morton SB, Baldassare M, Edlund T, Jessell TM, Pfaff SL. 1994. Topographic organization of embryonic motor neurons defined by expression of LIM homeobox genes. Cell 79:957–970.

Wang TF, Ding CN, Wang GS, Luo SC, Lin YL, Ruan Y, Hevner R, Rubenstein JL, Hsueh YP. 2004. Identification of Tbr-1/CASK complex target genes in neurons. J Neurochem 91:1483–1492.

Wichterle H, Turnbull DH, Nery S, Fishell G, Alvarez-Buylla A. 2001. In utero fate mapping reveals distinct migratory pathways and fates of neurons born in the mammalian basal forebrain. Development 128:3759–3771.

Wilbrecht L, Williams H, Gangadhar N, Nottebohm F. 2006. High levels of new neuron addition persist when the sensitive period for song learning is experimentally prolonged. J Neurosci 26:9135–9141.

Wild JM, Karten HJ, Frost BJ. 1993. Connections of the auditory forebrain in the pigeon (*Columba livia).* J Comp Neurol 337:32–62.

Wild JM, Williams MN, Howie GJ, Mooney R. 2005. Calcium-binding proteins define interneurons in HVC of the zebra finch (*Taeniopygia guttata).* J Comp Neurol 483:76–90.

Wilson CJ. 2004. Basal ganglia. In: Shepherd GM, editor. The synaptic organization of the brain, 5th ed. Oxford: Oxford University Press. p 361–413.

Xu Q, Cobos I, De La Cruz E, Rubenstein JL, Anderson SA. 2004. Origins of cortical interneuron subtypes. J Neurosci 24:2612–2622.

Yamamoto T, de Crombrugghe B, Pastan I. 1980. Identification of a functional promoter in the long terminal repeat of Rous sarcoma virus. Cell 22:787–797.

Yu AC, Margoliash D. 1996. Temporal hierarchical control of singing in birds. Science 273:1871–1875.